

# Temporal Variations In Vapor Intrusion-Induced Indoor Air Contaminant Concentrations

Jonathan G. V. Ström<sup>a</sup>, Yuanming Guo<sup>b</sup>, Yijun Yao<sup>b</sup>, Eric M. Suuberg<sup>a</sup>

<sup>a</sup>*Brown University, School of Engineering, Providence, RI, USA*

<sup>b</sup>*Arizona State University, School of Sustainable Engineering and the Building Environment, Tempe, AZ, USA*

---

## Abstract

Temporal variability in indoor air contaminant concentrations at vapor intrusion (VI) sites has been a concern for some time. We consider the source of the reported variability at VI sites located near Hill Air Force Base (AFB) in Utah, an EPA experimental house in Indiana, and Naval Air Station North Island in California. We focus in particular on how the indoor/outdoor pressure differences and air exchange rates affected indoor air contaminant concentrations at these sites. We investigate how these dynamics differ for a site that is characterized by a preferential pathway (like Hill AFB) and VI sites that are not influenced by such pathways, using three-dimensional fluid dynamics models and statistical analysis of the aforementioned sites. For a preferential pathway to impact a VI site, there must exist a medium allowing effective communication between a contaminant-delivering preferential pathway and the indoor air space, e.g. a permeable subslab space that may be provided by a gravel layer. At sites characterized by significant advective transport from the subslab to the indoor air space, much of the short-term variability in indoor air contaminant concentration can be explained by an impact of fluctuations in indoor/outdoor pressure differences. Meanwhile, air exchange rate variation drives most of the short-term variability at sites characterized by minor variations in advective transport.

*Keywords:* Vapor intrusion, Preferential pathways, Temporal variability, Attenuation factor, Air exchange rate, Indoor/outdoor pressure difference

---

---

*Email address:* `eric_suuberg@brown.edu` (Eric M. Suuberg)

## 1. Introduction

Long term vapor intrusion (VI) studies in both residential and larger commercial structures have raised concerns regarding significant observed transient behavior in indoor air contaminant concentrations[1, 2, 3, 4, 5, 6, 7]. Such variations make it difficult for those charged with protecting human health to formulate a response - should evaluation of the risk of exposure be based upon observed peak concentrations, or long-term averages, or something else? There is even uncertainty within the VI community regarding how to best develop sampling strategies to address this problem[1, 3, 8]. What represents a reasonable sampling strategy for a particular site a single 8-hour sample? Repeated 8-hour samples? Month-long samples? Continuous monitoring?

VI involves the migration of volatilizing contaminants from soil, groundwater or other subsurface sources into overlying structures. The basic nature of VI has been understood for some time and it has been the subject of much study, but some aspects remain poorly understood, such as the causes of the sometimes observed large temporal transients in indoor air concentrations. Results from a house operated by Arizona State University (ASU) near Hill AFB in Utah, an EPA experimental house in Indianapolis, IN and a large warehouse at the Naval Air Station (NAS) North Island, CA have all shown significant transient variations in indoor air contaminant concentrations. All were outfitted with sampling and monitoring equipment that allowed tracking temporal variation in indoor air contaminant concentrations on time scales of hours. All have shown that these concentrations vary significantly with time - orders of magnitude on the timescale of a day or days[9, 10, 5].

In one instance the source of the variation was clearly established during the study of the site. At the ASU house a drain pipe (or “land drain”) connected to a sewer system was discovered beneath the house. Careful isolation of this source led to a clear conclusion that this “preferential pathway” for contaminant vapor migration significantly contributed to observed indoor air contaminant levels and their fluctuations[10, 11]. While in this case the issue of a contribution from a preferential pathway was clearly resolved, what it left open was a question of whether existence of such a preferential pathway would always be expected to lead to large fluctuations in indoor air contaminant concentrations.

Similarly, a sewer pipe has recently been suggested to be a source of the contaminants found in the EPA Indianapolis house. That site was also char-

acterized by large indoor air contaminant concentration fluctuations[12, 7]. Sewer lines have been previously implicated as VI sources at several sites[13, 12, 14, 15]. A Danish study has estimated that roughly 20% of all VI sites in central Denmark involve significant sewer VI pathways[16]. Thus while consideration of sewer or other preferential pathways is now part of normal good practice in VI site investigation[1], it is still not known whether the existence of such pathways automatically means that large temporal fluctuations are necessarily to be expected.

In some of the above cited cases[13, 15], a sewer provided a pathway for direct entry of contaminant into the living space. While potentially important in many instances, this scenario is not further considered here where the focus is on pathways that deliver contaminant via the soil beneath a structure. It is, however, now known that even absent a preferential pathway, there may be significant transient variation in indoor air contaminant concentrations at VI sites[2, 17, 4]. One example is the site at NAS North Island at which no preferential pathways have been identified. Instead, a building at this site is characterized by significant temporal variations in indoor-outdoor pressure differential[5]. It is believed that this is the origin of the observed indoor air contaminant concentration fluctuations at that site.

This paper investigates the sources of the temporal variation in indoor air contaminant concentrations in both the presence and absence of preferential pathways. In this work, the latter scenarios are referred to as “normal” VI scenarios, in which there is typically a groundwater source of the contaminant. Specifically, we pose the question of just how much variation in indoor air contaminant concentration may be expected at such normal VI sites vs. those characterized by preferential pathways within the soil beneath the site. The conditions required for preferential pathways to become significant contributors to temporal variations in indoor air contaminant concentrations are also explored, and the consequences for sampling strategies are discussed.

## 2. Methods

### 2.1. Statistical Analysis Of Field Data

To frame the question of just how much variability in indoor air contaminant concentrations is actually observed, field datasets have been analyzed. For this purpose, datasets from the ASU house in Utah, the EPA Indianapolis site and North Island NAS were chosen for analysis. Read-

ers are referred to the original published works for details regarding data acquisition[9, 10, 3, 5, 7].

The ASU house data were obtained over a period of several years. During part of this time, controlled pressure method (CPM) tests were being conducted, in which the house was underpressurized to an extent greater than that characterizing “normal” house operation: increasing VI potential[18, 6, 9]. The period of CPM testing is thus excluded from the analysis. Likewise, the existence of a preferential pathway at the ASU house needs to be considered in examining that dataset; during some of the testing at that site, this pathway was cut off, resulting in “normal” VI conditions in which the main source of contaminant was diffusion of contaminant vapor from an underlying groundwater source.

The NAS North Island dataset has not (as far as is known) been influenced by a preferential pathway, but the structure there was subject to “large” internal pressure fluctuations. By “large” is meant still only of order 10-20 Pa, but these were greater than those generally recorded at the ASU house during normal operations. The underlying soil at NAS North Island is sandy[5] and more permeable than that at the ASU site, which will be shown to lead to greater pressure sensitivity in the former case.

The Indianapolis site investigation also spanned a number of years and periodically included the testing of a sub-slab depressurization system (SSD) for VI mitigation. Only the period before the installation of this system was considered in the present analysis. It is likely a sewer line beneath the structure acted as a preferential pathway[12]. Unlike at the ASU house, this preferential pathway was never removed or blocked, making it impossible to isolate the role of the preferential pathway at this site. It is still of interest to consider the data from this site because of the completeness and extensiveness of the data collection. Figure 1 illustrates a typical reported series of indoor air trichloroethylene (TCE) concentration measurements from this site. There is almost a two order of magnitude variation in the concentration data.

Some of the analysis of the above three field data sets relies on a probability density estimation technique called “kernel density estimation” (KDE). KDE is a technique used for estimating the probability distribution of a random variable(s) by using multiple kernels, or weighting functions to characterize the data sets. In this case, Gaussian kernels are used to create the KDEs. This means that it is presumed that the variables of interest (i.e., indoor air contaminant concentrations and indoor-outdoor pressure differ-

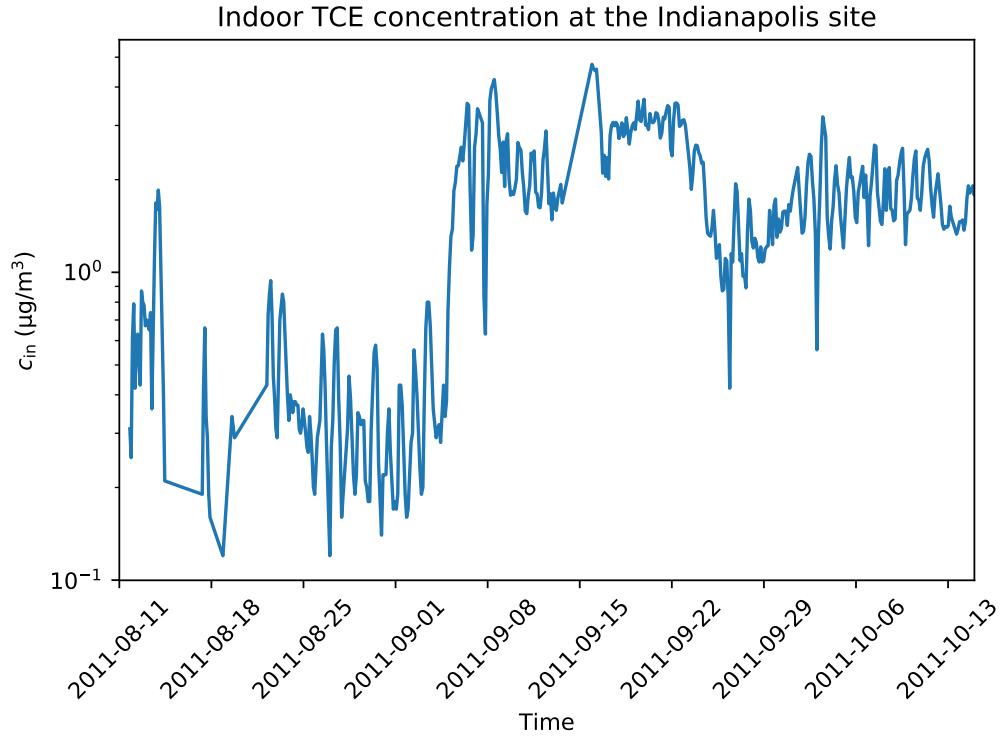


Figure 1: Typical data on indoor air TCE contaminant concentrations at the Indianapolis site[7].

entials, as sampled) are normally distributed around mean values and that there are statistical fluctuations associated with each sampling event. In this instance, the scipy statistical package was used to construct the KDEs, assuming a bandwidth parameter determined by Scott’s rule. The SciPy Python library was used to conduct all statistical analysis and data processing[19].

## 2.2. Modeling Work

A previously described three-dimensional computational fluid dynamics model of a generic VI impacted house has been used to elucidate certain aspects of transient VI processes. In the present work, there has been an addition of a preferential pathway to the “standard” model that has been described before in publications by this group[20, 21, 22]. As in the earlier studies, only the vadose zone soil domain is directly modeled. Figure 2 shows a cutaway view of the relevant modeling domain.

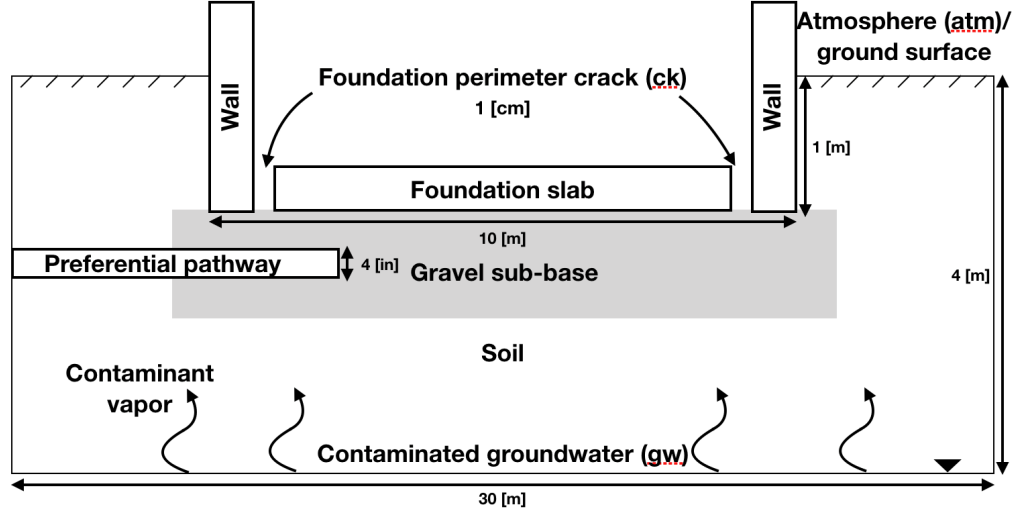


Figure 2: Foundation and vadose zone soil represented in the modeling. Note that here a gravel sub-base material is shown, but in certain simulations, that material is absent and the surrounding soil directly contacts the foundation slab. Different assumptions are made regarding the preferential pathway, here shown as a pipe entering the gravel sub-base. In some cases, the preferential pathway has been "turned off".

133 The modeled VI impacted structure is assumed to have a 10x10 m foun-  
 134 dation footprint, with the bottom of the foundation slab lying 1 m below  
 135 ground surface (bgs), simulating a house with a basement. The indoor air  
 136 space is modeled as a continuously stirred tank (CST)[1] and all of the con-  
 137 taminant entering the house is assumed to enter with soil gas through a 1  
 138 cm wide crack located between the foundation walls and the foundation slab  
 139 around the perimeter of the house. All of the contaminant leaving the in-  
 140 door air space is assumed to do so via air exchange with the ambient. The  
 141 indoor control volume is here assumed to consist of only of the basement,  
 142 having a total volume of 300 m<sup>3</sup>. Clearly different assumptions could be  
 143 made regarding the structural features and the size of the crack entry route,  
 144 but for present purposes, this is unimportant as the intent is only to show  
 145 for "typical" values what the influence of some critical parameters is.

146 The modeled surrounding soil domain extends 5 meters from the perime-  
 147 ter of the house and is assumed to consist of sandy loam, except as noted  
 148 otherwise. Directly beneath the foundation slab, there is assumed to be a 30  
 149 cm (one foot) thick gravel layer, except in certain cases here this sub-base

150 material is assumed to be the same as the surrounding soil (termed a "uni-  
 151 form" soil scenario). The groundwater beneath the structure is assumed to  
 152 be homogeneously contaminated with TCE selected as a prototypical con-  
 153 taminant. The groundwater itself is not modeled, as the bottom of the  
 154 model domain is defined by the top of the water table. Where relevant, the  
 155 preferential pathway is modeled as a 10 cm (4") pipe that opens into the  
 156 gravel sub-base beneath the structure. The air in the pipe is also assumed  
 157 to be contaminated with TCE at a vapor concentration equal to the vapor  
 158 in equilibrium with the groundwater contaminant concentration below the  
 159 structure, modified by a scaling factor  $\chi$  (allowing the contaminant concen-  
 160 tration in the pipe to be parameterized). This model illustrates the concept  
 161 of a "preferential pathway", as the pipe carries contaminant vapor to the  
 162 immediate vicinity of the foundation, by a path that circumvents the usual  
 163 soil diffusion pathway.

164 The ground surface and the pipe are both sources of air to the soil domain.  
 165 Both are assumed to exist at reference atmospheric pressure. Soil gas trans-  
 166 port is governed by Richard's equation, a modified version of Darcy's Law,  
 167 taking the variability of soil moisture in the vadose zone into account[23].  
 168 The van Genuchten equations are used to predict the soil moisture content  
 169 and thus the effective permeability of the soil[24]. The effective diffusivity  
 170 of contaminant in soil is calculated using the Millington-Quirk model[25].  
 171 The transport of contaminant vapor in the soil is assumed to be governed by  
 172 the advection-diffusion equation, in which either advection or diffusion may  
 173 dominate depending upon position and particular circumstances. The key  
 174 working equations and the boundary conditions are summarized in Table 1.

Governing Equations					
Unsteady-CST	$V \frac{dc_{in}}{dt} = \int_{A_{ck}} j_{ck} dA - c_{in} A_e V_{slab}$				
Richard's	$\nabla \cdot \rho \left( -\frac{\kappa_s}{\mu} k_r \nabla p \right) = 0$				
Transport	$\frac{\partial}{\partial t} \left( \theta_w c_w + \theta_g c \right) = \nabla (D_{eff} \cdot \nabla c) - \vec{u} \cdot \nabla c$				
Millington-Quirk	$D_{eff} = D_{air} \frac{\theta_g^{10/3}}{\theta_t^2} + \frac{D_{water}}{K_H} \frac{\theta_w^{10/3}}{\theta_t^2}$ $Se = \frac{\theta_w - \theta_r}{\theta_t - \theta_r} = [1 +  \alpha z ^n]^{-m}$				
van Genuchten	$\theta_g = \theta_t - \theta_w$ $k_r = (1 - Se)^l [1(Se^m)^m]^2$ $m = 1 - 1/n$				
Boundary Conditions					
Boundary	Richard's Eqn.		Transport Eqn.		
Foundation crack	$p = p_{in/out} \text{ (Pa)}$		$j_{ck} = \frac{uc}{1 - \exp(uL_{slab}/D_{air})}$		
Groundwater	<i>No flow</i>		$c = c_{gw} K_H \text{ (}\mu\text{g/m}^3\text{)}$		
Ground surface	$p = 0 \text{ (Pa)}$		$c = 0 \text{ (}\mu\text{g/m}^3\text{)}$		
Preferential pathway	$p = 0 \text{ (Pa)}$		$c = c_{gw} K_H \chi \text{ (}\mu\text{g/m}^3\text{)}$		
Soil Properties[26, 27, 28]					
Soil	$\kappa_s \text{ (m}^2\text{)}$	$\theta_s$	$\theta_r$	$\alpha \text{ (1/m)}$	$n$
Gravel	$1.3 \cdot 10^{-9}$	0.42	0.005	100	3.1
Sandy Loam	$5.9 \cdot 10^{-13}$	0.39	0.039	2.7	1.4
Trichloroethylene (diluted in air) Properties[27, 28]					
	$D_{air} \text{ (m}^2\text{/h)}$	$D_{water} \text{ (m}^2\text{/h)}$	$\rho \text{ (kg/m}^3\text{)}$	$\mu \text{ (Pa} \cdot \text{s)}$	$K_H$
	$2.47 \cdot 10^{-2}$	$3.67 \cdot 10^{-6}$	1.614	$1.86 \cdot 10^{-5}$	0.403
Building Properties					
	$V_{base} \text{ (m}^3\text{)}$	$L_{slab} \text{ (cm)}$	$A_e \text{ (1/hr)}$		
	300	15	0.5		

Table 1: Governing equations, boundary conditions & model input parameters. (See below for table of nomenclature).

### 175 3. Results & Discussion

#### 176 3.1. Variation In Indoor Air Contaminant Concentration Over Time

177 High frequency measurement of indoor air contaminant concentrations,  
178  $c_{in}$ , such as those in Figure 1, took place at both the ASU House and the



Indianapolis House over significant periods (Indianapolis: ca 1.7 years, ASU house: ca 3.5 years)[7, 3]. Furthermore, at the Indianapolis site  $c_{in}$  for three different contaminants, chloroform, TCE, and tetrachloroethylene (PCE) were all collected, allowing examination of the variability of each VI contaminant. The NAS North Island NAS dataset was obtained over a much shorter duration (9 days), and is therefore not examined in this portion of the analysis. It should also be noted that the ASU house used 4-hour sorbent tubes, while Indianapolis took instantaneous "grab" samples.

Figure 1 showed a large degree of temporal variation in one of the components, and the data for the other components were quite similar. What is apparent upon closer examination of such data is that the actual day-to-day variations are typically not nearly as large as those observed when tracking the data for a longer time. To demonstrate this point, the quotient of the maximum and minimum  $c_{in}$  values (denoted as  $c_{max}/c_{min}$ ) are shown as a function of time in Figure 3. The values shown in Figure 3 are the means of the quotients calculated for samples separated by the indicated times and the error bars indicate the 95th percentile of all the data points. Hypothetical resampling periods of one, two, three days, and the same number of weeks, and months were chosen.

For example, if the data are examined in terms of the mean maximum variation observable over the course of 24 hours (one day) the variation is no greater than about a factor of two for any of the contaminants at the Indianapolis house or for TCE at the ASU house (when the preferential pathway was closed). The mean variability at the latter was only a bit higher (about a factor of 3) when the preferential pathway was open. In other words, a sampling protocol that involves sampling on two consecutive days would typically not uncover the large temporal variations that characterize the site over longer periods of time. As Figure 1 shows, there are certainly isolated days in which a larger daily change was observed, but these were not typical, to the extent that they fall outside of the 95% criteria used in defining the error bars. So while such unusual jumps might be seen (for unknown reasons) in a very small percentage of cases, the expectation is much more represented by what is shown in Figure 3.

Weeks of temporal separation in sampling events are required to observe the large variations of concern. Orders of magnitude differences begin to manifest themselves over the course of months. This is not surprising, since those who performed the measurements have already reported that there were seasonal aspects to the values obtained. This would be consistent with

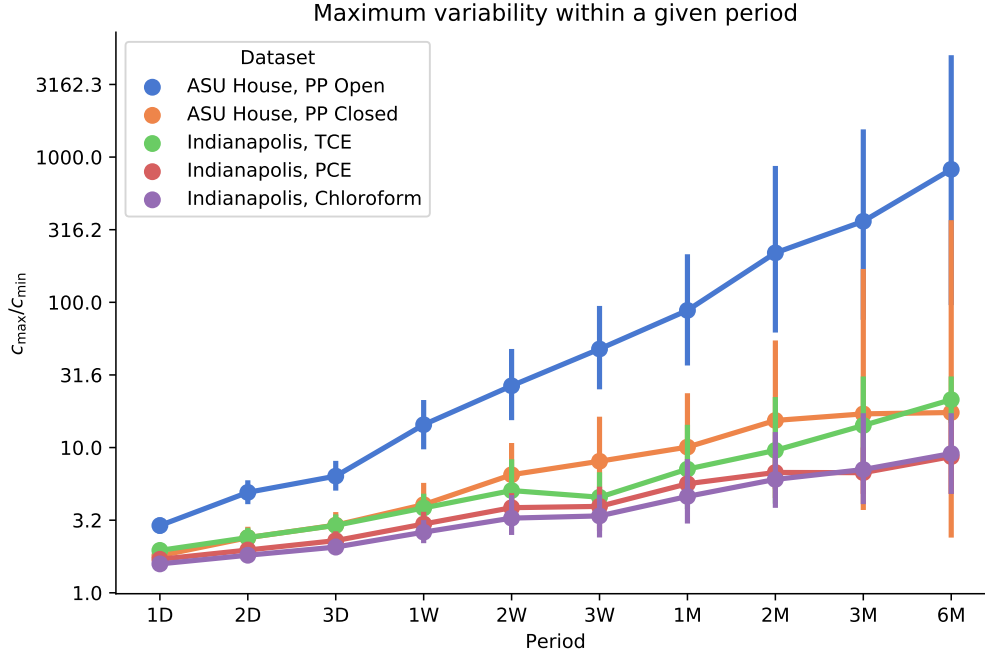


Figure 3: Mean values of the maximum change in indoor air contaminant concentration that may be expected over a given time period. (e.g., 1D is 1 day, 2W is 2 weeks, and 3M is 3 months). The error bars are the 95% confidence intervals.

217 requiring months to see the more significant variations.

218 This analysis also suggests that certain types of preferential pathways  
 219 contribute to larger variations on shorter timescales (ASU House). Even  
 220 though there was a preferential pathway present at the Indianapolis House,  
 221 the transients associated with its presence were of a slower nature and the  
 222 behavior was not unlike what was observed at ASU House when the preferential  
 223 pathway was closed. This warns that the mere existence of a preferential  
 224 pathway is not by itself sufficient to create a situation of large variations over  
 225 short sampling times.

226 The longer the resampling period, the larger the maximum variability  
 227 in observed indoor air contaminant concentrations. In the case of the ASU  
 228 House with the preferential pathway open, the variability went from less than  
 229 a threefold difference on the timescale of a day, to two to three orders of  
 230 magnitude over the course of weeks. Thus there are different timescales that  
 231 characterize different extents of variation, again pointing to the existence of

232 more than a single factor that determines variability.

233 Multiple samples taken over a short time period, e.g. a few days, are  
234 unlikely to uncover significant variation in indoor air contaminant concen-  
235 tration; the larger transient variations typically manifest after longer time  
236 periods.

### 237 3.2. Statistical Analysis of Field Data

238 The data in Figure 1 and Figure 3 raise the question of what then actually  
239 determines the large degree of temporal variation sometimes reported. The  
240 rate of advective entry of soil gas into a structure is frequently cited as playing  
241 an important role in determining entry rate of contaminant. This advective  
242 entry rate is closely linked to the indoor-outdoor pressure difference, as can  
243 be caused by the “stack effect”, for example. Thus we first consider how much  
244 variability there might be in the pressure driving force for advection, and if  
245 this can explain the observed variability in observed indoor air contaminant  
246 concentrations.

247 The pressure difference between the indoor and outdoor/ambient ( $p_{\text{in/out}}$ )  
248 leads to advection, by which contaminants are drawn into (or prevented from)  
249 entering a structure. Changes in  $p_{\text{in/out}}$  can take place quickly, leaving open  
250 the possibility of their impacting VI far more rapidly than can fluctuations in  
251 say groundwater depth or contaminant concentration (these latter processes  
252 take weeks or even months to impact the overlying structure).

253 We examine the relationship between  $p_{\text{in/out}}$  and  $c_{\text{in}}$  by constructing the  
254 two-dimensional kernel density estimation (KDE) plots seen in Figure 4. The  
255 KDE plots allow us to view the measured distributions of  $p_{\text{in/out}}$  and  $c_{\text{in}}$ , and  
256 develop a visual impression of how well these distributions correlate with one  
257 another. For this analysis we considered two VI sites, NAS North Island and  
258 the ASU House. The ASU House dataset was divided into two periods, one  
259 before and the other after the land drain (called the preferential pathway  
260 (PP) from here on) had been closed. By comparing these two periods on a  
261 single plot, the impact of the preferential pathway becomes clearer.

262 In Figure 4, the indoor air contaminant concentration  $c_{\text{in}}$  is normalized to  
263 the mean  $c_{\text{in,mean}}$  of each dataset, allowing comparison of the impact  $p_{\text{in/out}}$   
264 on  $c_{\text{in}}$  independently from the large differences in absolute values of indoor  
265 air concentrations at the different sites. A value of 10 on the y-axis indicates  
266 that the corresponding plotted value of  $c_{\text{in}}$  is 10 times greater than the mean  
267 for the dataset, and 0.1 indicate that it is one tenth of the mean.

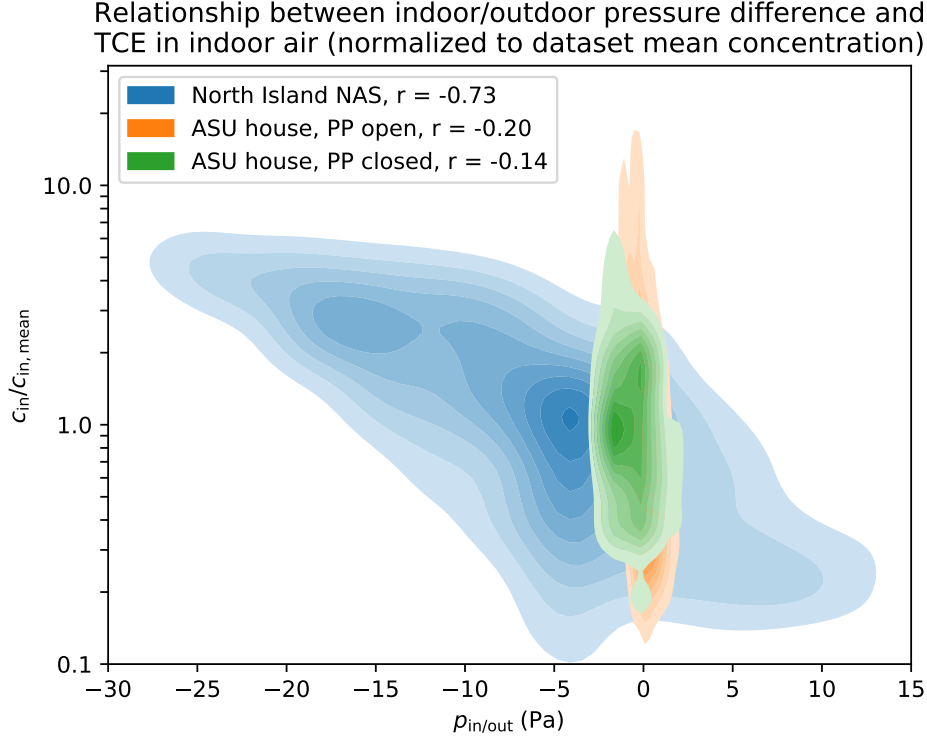


Figure 4: 2D-KDE plot showing the distributions of indoor air contaminant concentration, the indoor/outdoor pressure difference, and how they correlate to each other.

	North Island NAS		ASU House PP Open		ASU House PP Closed	
Percentile	5th	95th	5th	95th	5th	95th
$p_{in/out}$ (Pa)	-19.9	7.4	-1.4	2.1	-2.1	2.27
$c_{in}/c_{in,mean}$	4.1	0.2	13.5	0.2	3.3	0.4

Table 2: 5th and 95th percentile values of  $p_{in/out}$  and  $c_{in}/c_{in,mean}$  in Figure 4.

268 Inspection of the range of normalized  $c_{in}$  values in Figure 4 again shows  
 269 the two order of magnitude spread in observed values, implying a sampling  
 270 at one particular time might give a value that is two orders of magnitude  
 271 different than a result from a different time. Such issues have of course  
 272 already been pointed out by the investigators who obtained the data.

273 The power of this KDE representation is that it permits evaluation of the  
 274 relationship of two independently measured data - the indoor air contaminant  
 275 concentration and the indoor-outdoor pressure difference. Examining the  
 276 data in this manner immediately points to an important difference between  
 277 the data from the ASU House and those from NAS North Island. At NAS  
 278 North Island site  $p_{\text{in/out}}$  varies significantly; the 5th and 95th percentile of  
 279  $p_{\text{in/out}}$  are -19.9 and 7.4 Pa respectively. This may be contrasted with 5th  
 280 and 95th percentile  $p_{\text{in/out}}$  at the ASU house: -1.4 and 2.1 Pa (with the PP  
 281 open), and -2.1 and 2.27 Pa (PP closed).

282 The much larger under- and overpressurization of the NAS North Island  
 283 site compared to the ASU House makes the pressure dependence of indoor  
 284 air concentration much more visible at the former site. The Pearson's r-value  
 285 for the correlation between  $p_{\text{in/out}}$  and  $c_{\text{in}}$  for each dataset is shown in the  
 286 legend, and confirms what is apparent to the eye; the pressure driving force is  
 287 a determining factor for observed contamination at NAS North Island. But  
 288 the broadness of the band of the NAS North Island concentration data set  
 289 suggests that there is still a source of variability in  $c_{\text{in}}$  that has not been fully  
 290 captured - this will be addressed below.

291 The ASU house datasets offer a different picture. The variability of  $c_{\text{in}}$  is  
 292 just as large, or even larger than at NAS North Island, yet the  $p_{\text{in/out}}$  varied  
 293 far less. The weaker dependence of  $c_{\text{in}}$  on the pressure difference is confirmed  
 294 by the much lower r-values for the correlations between the variables. In  
 295 other words, there is not nearly as strong a correlation between variation in  
 296 indoor air contaminant concentration and pressure difference for the ASU  
 297 House as there was for NAS North Island. These results strongly suggest  
 298 that there are other factors besides indoor pressure determining indoor air  
 299 contaminant concentrations, and their variations, that may not be accounted  
 300 for in applying this method.

301 The data for the ASU House also offer an insight into the role of the  
 302 preferential pathway. At first glance it may seem like the  $c_{\text{in}}$  values for the  
 303 periods when the PP is open and closed are relatively comparable. However,  
 304 the 5th and 95th percentiles values of  $c_{\text{in}}/c_{\text{in,mean}}$  differ significantly as may  
 305 be seen in Table 2. It is clear that existence of the preferential pathway  
 306 dramatically increases the variability in indoor air contaminant concentra-  
 307 tion. This again is entirely consistent with what the investigators of that  
 308 site have already reported[11]. The correlation with indoor-outdoor pressure  
 309 difference is weak in the ASU house cases, so there are clearly factors other  
 310 than pressure difference that determine the variability in each. These will be

311 explored with the help of a modeling analysis presented below.

### 312 3.3. Variability Of Attenuation to Subslab Concentrations

313 Observed temporal variations in indoor air contaminant concentrations  
314 might be explained by temporal variations in subslab contaminant concen-  
315 trations. To examine how variability in subslab contaminant concentration  
316 might contribute to variability in indoor air contaminant concentration, data  
317 on the attenuation from subslab ( $\alpha_{\text{subslab}} = c_{\text{in}}/c_{\text{subslab}}$ ) were examined. The  
318 dataset utilized for this was that from the ASU House. The  $c_{\text{subslab}}$  values  
319 were taken from a soil gas probe labeled as "6" at the ASU house. This probe  
320 was located closest to both the exit of the preferential pathway pipe, and to  
321 a reported breach in the foundation that served as a key entry pathway for  
322 contaminant getting into the house[11]. The results are shown in Figure 5,  
323 which shows the full distributions for both the case in which the preferential  
324 pathway was "open" and when it "closed".

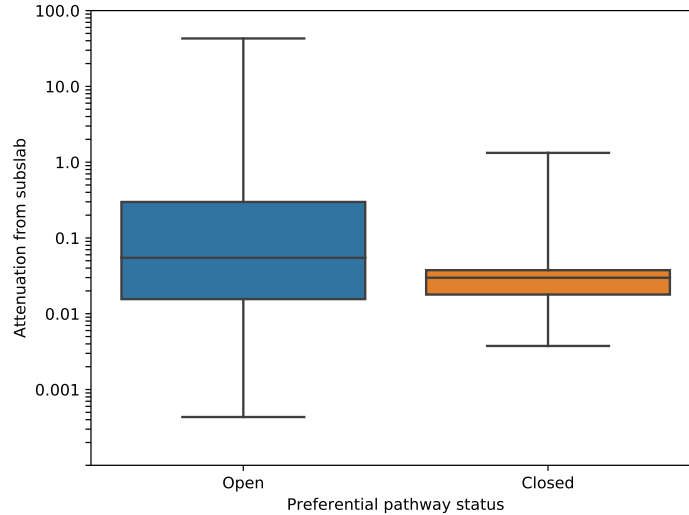


Figure 5: Boxplot of  $\log_{10}$  (subslab to indoor air contaminant attenuation) at the ASU house site. The box shows the quartiles of the distribution, the whiskers the extent of the distribution.

325 It is apparent that during the period when the preferential pathway was  
326 closed,  $\alpha_{\text{subslab}}$  did not vary significantly, and was quite close to the EPA  
327 recommended  $\alpha_{\text{subslab}}$  value of 0.03[1]. Thus during the period when the

328 preferential pathway was closed, large temporal variations in subslab concen-  
329 trations could not have been driving the variations in indoor air contaminant  
330 concentrations.

331 When the PP was open, there was considerably more variability in the  
332 subslab concentration values, and the mean value was higher than in the  
333 case where the preferential pathway was closed. It was also not uncommon  
334 for the observed  $\alpha_{\text{subslab}}$  to exceed unity. While large  $\alpha_{\text{subslab}}$  values may  
335 sometimes indicate indoor sources at a site, there were none at the ASU  
336 house. A more likely explanation is that even though probe "6" was located  
337 in close proximity to the exit of the preferential pathway, there might have  
338 still existed significant spatial variability in  $c_{\text{subslab}}$  that could not be captured  
339 with a single measurement. This suggests caution is needed in profiling  
340 subslab contaminant concentrations in the presence of preferential pathways  
341 - significant variations are possible.

342 What the results of Figure 5 do clearly show is that the existence of a  
343 preferential pathway of the kind at ASU House (and idealized in Figure 1)  
344 can influence the temporal variation of subslab concentrations in a much less  
345 predictable way than those observed in "normal" VI scenarios.

### 346 3.4. Modeling Results

#### 347 3.4.1. Pressure Effects

348 Having established the potential impacts of certain inputs on determining  
349 variability in indoor air contaminant concentrations, the mathematical model  
350 of VI can help further elucidate other key aspects. The results of calculations  
351 on a scenario corresponding to Figure 2 are presented in Figure 6. This  
352 scenario is not intended to exactly represent the situation at ASU House,  
353 but it is similar in the key aspect of having a preferential pathway delivering  
354 contaminant to a gravel sub-base. The full, complex geometry of the ASU  
355 House has not been represented, but the modeled structure is of comparable  
356 size, and will be subject to operational parameters based upon what were  
357 measured at that site. The general modeling conditions are those shown in  
358 Table 1.

359 In the calculation results shown in the top panel of Figure 6, a prefer-  
360 ential pathway is assumed to provide air containing contaminant vapor at  
361 a concentration equivalent to the vapor in equilibrium with the underlying  
362 groundwater source. Here, the indoor air exchange rate  $A_e$  was assumed to  
363 be a constant 0.5 per hour, and  $p_{\text{in/out}}$  was varied from -5 to 5 Pa. Values  
364 of predicted indoor air contaminant concentrations,  $c_{\text{in}}$  were obtained from

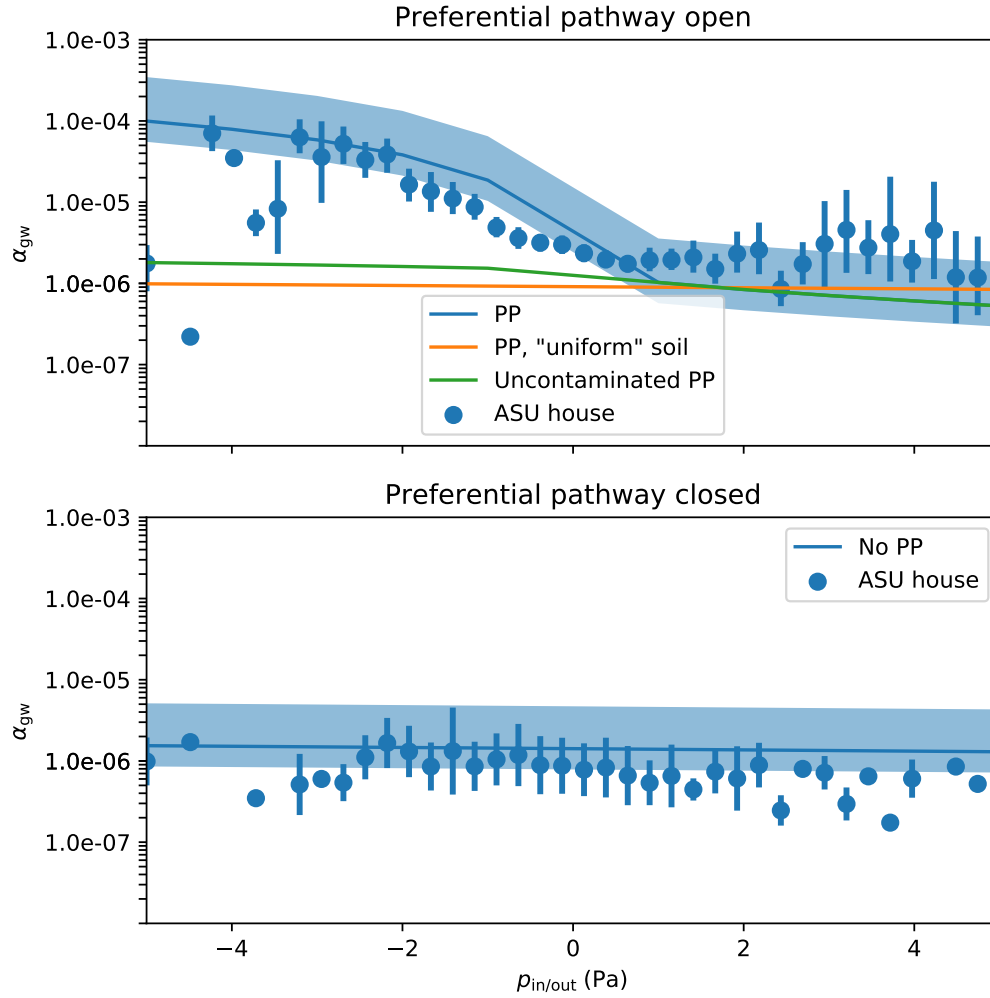


Figure 6: Simulated preferential pathway scenarios compared to actual ASU house field data. Field data are binned in 40 evenly spaced pressure bins, with the dot representing the mean and errors bars the 95% confidence interval of data at a particular pressure range. Shaded blue represent the range of model predictions for the indicated pressure difference, due to air exchange rate variability (using 5th and 95th percentile values of measured exchange rates). Top panel is for various cases representing an "open" preferential pathway, the lower panel with the pathway "closed".

365 steady state calculations. The predicted  $c_{in}$  values were then normalized by  
 366 the assumed vapor concentration in equilibrium with groundwater  $c_{gw}$ , giving  
 367 the attenuation from groundwater  $\alpha_{gw}$ . The predicted values of  $\alpha_{gw}$  as a



function of  $p_{\text{in/out}}$  are given by the central blue line in the upper panel of Figure 6. These predicted values are compared to actual measured  $\alpha_{\text{gw}}$  values from the ASU House for the period during which the preferential pathway was open (blue points).

The model successfully predicts the observed trends in  $\alpha_{\text{gw}}$  as  $p_{\text{in/out}}$  decreases (increased depressurization) but somewhat underpredicts  $\alpha_{\text{gw}}$  as the house is overpressurized. Most significantly, the model captures that even for a small increase in depressurization (0 to -5 Pa) a very large increase in  $\alpha_{\text{gw}}$  (two order of magnitude) can occur.

The asymmetry relative to the predictions for depressurization and overpressurization is due to two factors. First, the preferential pathway acts not only as a source of contaminant vapor, but also as a source of air to the subslab. Because of the large resistance to soil gas flow in the surrounding soil, having a local source of air to support the increase of advective flow into the structure from the subslab region makes a large difference.

The above was proven by a second simulation, where the model was rerun with the preferential pathway present, but with the permeable (gravel) layer in the subslab removed and replaced by the surrounding soil (sandy loam). This gave a "uniform soil" scenario the results of which are shown as an orange line in the top panel of Figure 6. This simulation demonstrates that without a permeable subslab to effectively allow the "advective potential" to be realized, existence of preferential pathway will actually not impact a VI site very much. In order for a preferential pathway to significantly contribute to VI, this requires a scenario involving good advective communication between it the indoor environment. These requirements were met at the ASU House.

A perhaps obvious second requirement is that the preferential pathway must deliver contaminant vapors to be impactful. In another simulation, the permeable (gravel) subslab region was included, but the preferential pathway merely delivered clean air to the subslab. The result of this simulation is shown as the green line in the top panel of Figure 6. This shows that while there was a lightly larger  $\alpha_{\text{gw}}$  compared to the "uniform soil" scenario, it is nowhere near as significant as when the preferential pathway delivers contaminant vapors. The contaminated and uncontaminated preferential pathway scenarios (blue and green lines respectively) thus bound the range of  $\alpha_{\text{gw}}$  that would be observed for a given  $p_{\text{in/out}}$  depending on the contaminant vapor concentration in the preferential pathway.

The model is also able to capture the weak trend in  $\alpha_{\text{gw}}$  with  $p_{\text{in/out}}$  when

406 a preferential pathway is absent, but when there still exists a permeable  
 407 subslab region. These results are shown in the bottom panel of Figure 6.  
 408 These results are again in agreement with what was observed at the ASU  
 409 House when the preferential pathway was closed, i.e. that there was a much  
 410 more modest variation in indoor air concentration, irrespective of pressure,  
 411 when the preferential pathway was cut off.

412 The above simulations capture the trend in  $\alpha_{\text{gw}}$  with  $p_{\text{in/out}}$  but do not yet  
 413 capture the full variability of the concentration results over the "most prob-  
 414 able" portion of observed pressure distributions shown in Figure 4 (which  
 415 tend to be from -2 to +2 Pa). The results of Figure 6 show a spread of  
 416 almost an order of magnitude over this pressure range for the case of the  
 417 "open" preferential pathway, and almost no spread at all when the prefer-  
 418 ential pathway is "closed". Hence the predicted variability is roughly an  
 419 order of magnitude too low, when considering only the influence of pressure.  
 420 There is a factor that tends to increase the spread of the data one additional  
 421 order of magnitude beyond what was predicted by the base calculations of  
 422 Figure 6. We believe that it is variations in air exchange rate, operating in  
 423 concert with the natural variations in pressure differential, that explain the  
 424 remaining variability.

### 425 3.4.2. Air Exchange Rate Effects

426 Table 3 shows the observed variations in air exchange rates for the ASU  
 427 House and Indianapolis House, compared with EPA's summary of the dis-  
 428 tribution of typical residential air exchange rates[29, 30]. Examination of  
 429 these distributions point in a clear direction for modifying the above model.  
 430 Instead of using a constant value of air exchange rate, as is customary, its  
 431 values should be parameterized. A higher air exchange would of course be  
 432 associated with lower  $c_{\text{in}}$  and vice versa. Moreover,  $A_e$  may sometimes be  
 433 correlated with  $p_{\text{in/out}}$ . Determining any general relationship between  $A_e$  and  
 434  $p_{\text{in/out}}$  is difficult: the structure itself and weather phenomena have a signifi-  
 435 cant effect on air exchange. As the data in Figure 7 show, there is no easily  
 436 discernable correlation between these variables at the ASU site, though there  
 437 is a hint of slight seasonal dependence. Note: a relationship between  $A_e$  and  
 438  $p_{\text{in/out}}$  may be established for larger  $p_{\text{in/out}}$  via the building leakage curves,  
 439 which are widely used for heating, ventilation and air conditioning systems  
 440 in construction.

441 To show the influence of possible statistical fluctuations of air exchange  
 442 rate on the predictions of  $\alpha_{\text{gw}}$  values, the scenarios of Figure 6 were rerun

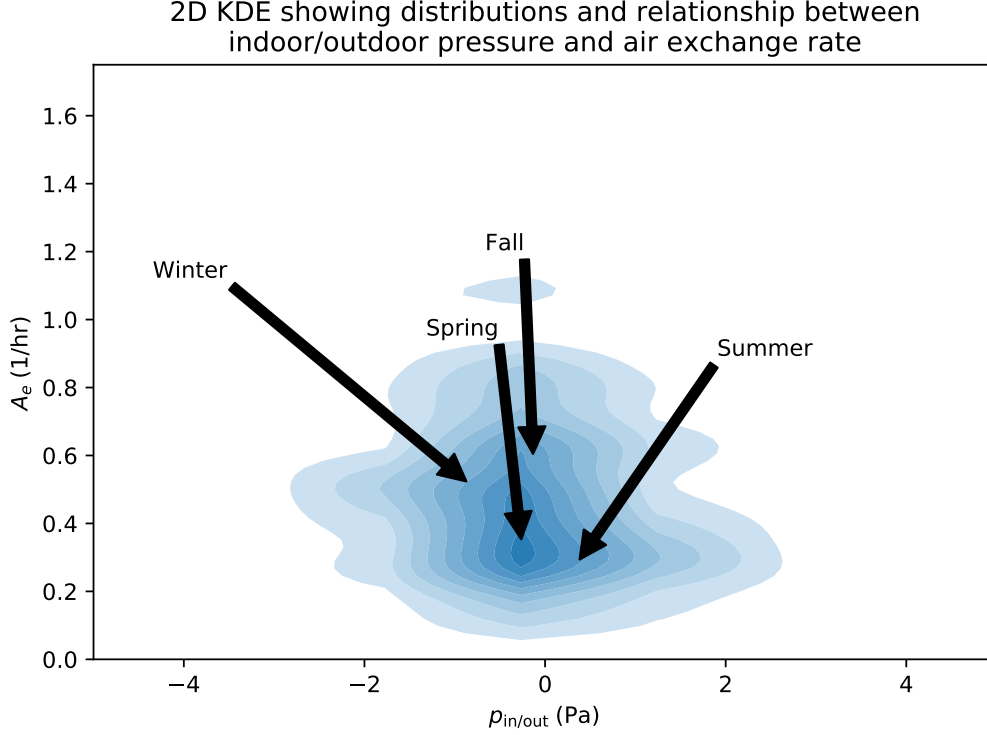


Figure 7: 2D KDE figure showing distributions and relationship between indoor/outdoor pressure difference and air exchange rate. The seasonal median  $p_{\text{in/out}}$  and  $A_e$  are indicated by the location of the respective arrow tips. Only non-CPM period considered.

Percentile	10th	50th	90th
EPA[29, 30]	0.16-0.2	0.35-0.49	1.21-1.49
ASU house[3, 11]	0.21	0.43	0.78
Indianapolis[7]	0.34	0.74	1.27

Table 3: Air exchange rate values (1/hr)

443 calculated using the 5th and 95th percentile measured  $A_e$  values, 0.17 and  
 444 0.90 respectively (based upon the actual distributions in Figure S1), provid-  
 445 ing predicted upper and lower bounds for  $\alpha_{\text{gw}}$ . These bounds are indicated  
 446 by the shaded blue regions around the center line calculated for an assumed  
 447 constant  $A_e$  of 0.5 per hour.

448 It is apparent that assuming variability in air exchange rate allows cap-

449 turing most of the observed variability in  $\alpha_{\text{gw}}$ . We believe that this explains  
 450 the portion of the variation in indoor air contaminant concentration data  
 451 that cannot be explained by either existence of preferential pathways or by  
 452 the range in indoor depressurization. Thus, we believe that it is the inter-  
 453 play of preferential pathway conditions, with indoor pressure variations and  
 454 normal air exchange rates that help to explain the observations of significant  
 455 variations in reported indoor air contaminant concentrations.

### 456 3.4.3. Results of Transient Simulations

457 The above analyses have been conducted under simulated steady state  
 458 conditions. The conclusions regarding the importance of the different pa-  
 459 rameters are now examined in actual transient simulations. The model con-  
 460 figuration of Figure 2 is run in 24-hour transient simulations to examine how  
 461  $c_{\text{in}}$  fluctuates over the course of a "typical" day. The simulations vary  $p_{\text{in/out}}$   
 462 as one model input, and then assume either a constant or time-varying air  
 463 exchange rate,  $A_e$ . The ASU House dataset was again the source of the "typ-  
 464 ical"  $p_{\text{in/out}}$  temporal variation, obtained by examining the median, hourly,  
 465 diurnal  $p_{\text{in/out}}$  during the non-CPM periods. The statistically "typical"  $p_{\text{in/out}}$   
 466 cycle may be seen in the upper left panel of Figure 8 (note that values be-  
 467 tween the hourly median values are interpolated using cubic splines). The  
 468 "typical" air exchange rate is calculated in exactly the same way and is shown  
 469 by the blue line in the upper right panel of Figure 8. The orange line is the  
 470 air exchange rate value assumed for the calculations at constant air exchange  
 471 rate.

472 The result of these simulations are shown in the bottom two panels of  
 473 Figure 8, where the left and right panels show the results of open and closed  
 474 preferential pathways, respectively. The "max change" value in the legends  
 475 is the quotient of the lowest and highest predicted concentrations, i.e. a value  
 476 of two indicate that the maximum daily concentration is twice as high as the  
 477 lowest. This quantity may be compared with the value that is plotted for  
 478 "one day" in Figure 3. When the preferential pathway is open, there is a  
 479 maximum daily variation of roughly a factor of 5, irrespective of whether  $A_e$   
 480 fluctuates or not, which is somewhat more than the maximum daily varia-  
 481 tion shown in Figure 3. The relatively small difference between the variable  
 482 and constant  $A_e$  cases indicates that most of the variability during a "typi-  
 483 cal" day is here attributable to fluctuations in  $p_{\text{in/out}}$ , i.e. the contaminant  
 484 transport into the modeled structure is advection dominated. Even for the  
 485 small fluctuations in  $p_{\text{in/out}}$  the contaminant entry rate fluctuation drives

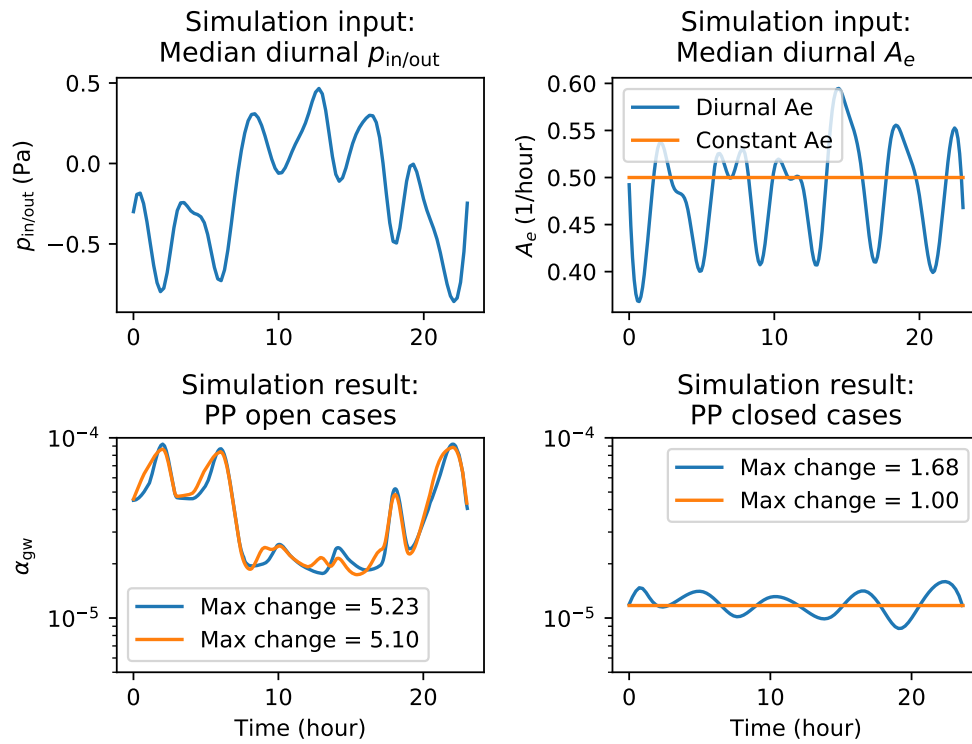


Figure 8: Transient simulation of a "typical" VI day, using diurnal indoor/outdoor pressure difference and air exchange rate as inputs. Effect of preferential pathway considered.

the observed indoor concentration. When the preferential pathway is closed the story is quite different. When air exchange rate is held constant, there is essentially no variation in  $c_{in}$ . This is again not surprising, as Figure 6 demonstrated that when the preferential pathway is closed, the influence of  $p_{in/out}$  on contaminant entry rate (and subsequently  $c_{in}$ ) is small. Combined with the small  $p_{in/out}$  this indicates that the contaminant transport into the modeled structure in this scenario is dominated by diffusion. When the air exchange rate is allowed to fluctuate, the maximum daily variation in  $c_{in}$  is 1.68, which is in line with what is shown in Figure 3. This shows that for a "typical" day, when the preferential pathway is closed off, much of the daily variation in  $c_{in}$  is due to daily fluctuations in air exchange rate.

These results demonstrate the complicated nature of temporal variability in  $c_{in}$ . It is important to recall that only the effects of indoor/outdoor pressure difference and air exchange rate have been considered here, but slower processes, e.g. changes in groundwater contaminant concentration or various seasonal effects can also have a significant impact on VI over time. For the shorter time periods of concern in recent studies of temporal variability in indoor contaminant concentrations we believe that these are dominated by combinations of indoor/outdoor pressure differentials and air exchange rate. For a site where advective communication between the subsurface and the indoor is good,  $p_{in/out}$  is likely a significant determinant of  $c_{in}$  and its temporal variability. We have shown that that such a scenario may arise due to a preferential pathway entering a permeable sub-base, but may also exist even in the absence of a preferential pathway just as the results from NAS North Island demonstrate. At sites where advective transport into the structure is limited, much of the temporal variability in  $c_{in}$  may be attributed to natural fluctuations in air exchange rate.

#### 4. Conclusions

Based on the statistical analysis of the field data presented, as well as the modeling efforts the following conclusions may be drawn.

- Indoor air contaminant concentrations are unlikely to vary by more than a factor of three over a week-long period if the site is not characterized by a preferential pathway, such as the one found at the ASU house site; else more than an order magnitude variability within the same period may be expected.

- 521 • Preferential pathways can cause significant spatial variability in the  
522 subslab. Subsequently, subslab vapor samples may reveal that the at-  
523 tenuation from subslab may significantly exceed the EPA recommended  
524 value of 0.03 and even exceed unity - potentially leading to the erro-  
525 neous conclusion that an indoor source is present.
- 526 • Preferential pathways such as the one found at the ASU house signif-  
527 icantly increase the advective transport potential through the founda-  
528 tion breaches at a site. This relies on effective communication between  
529 the indoor air space and the preferential pathway, e.g. a permeable  
530 subslab region (gravel layer) must exist.
- 531 • Sites characterized by significant advective potential, such as North  
532 Island NAS or the ASU house with the preferential pathway open,  
533 most of the short-term indoor air contaminant concentration variability  
534 may be attributed to fluctuations in indoor/outdoor pressure difference;  
535 at sites where the advective potential is low, e.g. ASU house with  
536 the preferential pathway closed, short-term variability is dominated by  
537 fluctuations in air exchange rate.

## 538 **Acknowledgements**

539 This project was supported by grant ES-201502 from the Strategic Envi-  
540 ronmental Research and Development Program and Environmental Security  
541 Technology Certification Program (SERDP-ESTCP).

---

$A_{\text{ck}}$	Crack area
$A_e$	Air exchange rate
$\alpha, n, m, l$	van Genuchten parameters
$\alpha_{\text{gw}}$	Attenuation from groundwater contaminant vapor source
$c_{\text{in}}$	Indoor air contaminant concentration
$c$	Soil-gas contaminant concentration
$c_w$	Soil-water contaminant concentration
$c_{\text{gw}}$	Contaminant groundwater concentration
$\chi$	PP contaminant concentration scaling parameter
$D_{\text{eff}}$	Effective diffusion coefficient
$D_{\text{air}}$	Diffusion coefficient in air
$D_{\text{water}}$	Diffusion coefficient in water
$\dot{j}_{\text{ck}}$	Contaminant molar flux through the foundation crack
$\kappa_s$	Saturated soil permeability
$K_H$	Dimensionless Henry's law constant
$k_r$	Relative permeability
$L_{\text{slab}}$	Thickness of the foundation slab
$M$	Molar mass
$\mu$	Contaminant vapor viscosity
NAS	Naval Air Stations
$p$	Pressure in soil
$p_{\text{in/out}}$	Indoor/outdoor pressure difference
PP	Preferential pathway
$\rho$	Density
Se	Soil water saturation
$t$	time
$\theta_g$	Vapor/gas filled porosity
$\theta_w$	Water filled porosity
$\theta_r$	Residual water filled porosity
$\theta_t$	Total porosity
$\vec{u}$	Soil-gas velocity (vector quantity)
VI	Vapor intrusion
$V_{\text{base}}$	Basement volume
$z$	Elevation above groundwater

---

Table 4: List of abbreviations and nomenclature



542 **References**

- 543 [1] U.S. Environmental Protection Agency, OSWER Technical Guide for  
544 Assessing and Mitigating the Vapor Intrusion Pathway From Subsurface  
545 Vapor Sources To Indoor Air, 2015.
- 546 [2] D. Folkes, W. Wertz, J. Kurtz, T. Kuehster, Observed Spatial and  
547 Temporal Distributions of CVOCs at Colorado and New York Vapor  
548 Intrusion Sites, *Ground Water Monitoring & Remediation* 29 (2009)  
549 70–80.
- 550 [3] C. Holton, H. Luo, P. Dahlen, K. Gorder, E. Dettenmaier, P. C. Johnson,  
551 Temporal Variability of Indoor Air Concentrations under Natural Con-  
552 ditions in a House Overlying a Dilute Chlorinated Solvent Groundwater  
553 Plume, *Environmental Science & Technology* 47 (2013) 13347–13354.
- 554 [4] J. E. Johnston, J. M. Gibson, Spatiotemporal variability of tetra-  
555 chloroethylene in residential indoor air due to vapor intrusion: A lon-  
556 gitudinal, community-based study, *Journal of Exposure Science and*  
557 *Environmental Epidemiology* 24 (2014) 564.
- 558 [5] V. Hosangadi, B. Shaver, B. Hartman, M. Pound, M. L. Kram, C. Fres-  
559 cura, High-Frequency Continuous Monitoring to Track Vapor Intrusion  
560 Resulting From Naturally Occurring Pressure Dynamics, *Remediation*  
561 *Journal* 27 (2017) 9–25.
- 562 [6] T. McHugh, P. Loll, B. Eklund, Recent advances in vapor intrusion  
563 site investigations, *Journal of Environmental Management* 204 (2017)  
564 783–792.
- 565 [7] U.S. Environmental Protection Agency, Assessment of Mitigation Sys-  
566 tems on Vapor Intrusion: Temporal Trends, Attenuation Factors, and  
567 Contaminant Migration Routes under Mitigated And Non-mitigated  
568 Conditions, 2015.
- 569 [8] P. C. Johnson, C. W. Holton, Y. Guo, P. Dahlen, E. H. Luo, K. Gorder,  
570 E. Dettenmaier, R. E. Hinchee, Integrated Field-Scale, Lab-Scale, and  
571 Modeling Studies for Improving Our Ability to Assess the Groundwater  
572 to Indoor Air Pathway at Chlorinated Solvent-Impacted Groundwater  
573 Sites, 2016.

- 574 [9] C. W. Holton, Evaluation of Vapor Intrusion Pathway Assessment  
575 Through Long-Term Monitoring Studies, PhD Thesis, Arizona State  
576 University, 2015.
- 577 [10] Y. Guo, Vapor Intrusion at a Site with an Alternative Pathway and a  
578 Fluctuating Groundwater Table, PhD Thesis, Arizona State University,  
579 2015.
- 580 [11] Y. Guo, C. Holton, H. Luo, P. Dahlen, K. Gorder, E. Dettenmaier,  
581 P. C. Johnson, Identification of Alternative Vapor Intrusion Pathways  
582 Using Controlled Pressure Testing, Soil Gas Monitoring, and Screening  
583 Model Calculations, *Environmental Science & Technology* 49 (2015)  
584 13472–13482.
- 585 [12] T. McHugh, L. Beckley, T. Sullivan, C. Lutes, R. Truesdale, R. Uppen-  
586 camp, B. Cosky, J. Zimmerman, B. Schumacher, Evidence of a sewer  
587 vapor transport pathway at the USEPA vapor intrusion research duplex,  
588 *Science of The Total Environment* 598 (2017) 772–779.
- 589 [13] K. G. Pennell, M. K. Scammell, M. D. McClean, J. Ames, B. Weldon,  
590 L. Friguglietti, E. M. Suuberg, R. Shen, P. A. Indeglia, W. J. Heiger-  
591 Bernays, Sewer Gas: An Indoor Air Source of PCE to Consider During  
592 Vapor Intrusion Investigations, *Groundwater Monitoring & Remedia-*  
593 *tion* 33 (2013) 119–126.
- 594 [14] M. Roghani, O. P. Jacobs, A. Miller, E. J. Willett, J. A. Jacobs, C. R.  
595 Viteri, E. Shirazi, K. G. Pennell, Occurrence of chlorinated volatile  
596 organic compounds (VOCs) in a sanitary sewer system: Implications  
597 for assessing vapor intrusion alternative pathways, *Science of The Total*  
598 *Environment* 616-617 (2018) 1149–1162.
- 599 [15] C. E. Riis, A. G. Christensen, M. H. Hansen, H. Husum, M. Terkelsen,  
600 Vapor intrusion through sewer systems: Migration pathways of chlori-  
601 nated solvents from groundwater to indoor air, 2010.
- 602 [16] K. B. Nielsen, B. Hvidberg, Remediation techniques for mitigating vapor  
603 intrusion from sewer systems to indoor air, *Remediation Journal* 27  
604 (2017) 67–73.

- 605 [17] D. Brenner, Results of a Long-Term Study of Vapor Intrusion at Four  
606 Large Buildings at the NASA Ames Research Center, *Journal of the*  
607 *Air & Waste Management Association* 60 (2010) 747–758.
- 608 [18] T. E. McHugh, L. Beckley, D. Bailey, K. Gorder, E. Dettenmaier,  
609 I. Rivera-Duarte, S. Brock, I. C. MacGregor, Evaluation of Vapor In-  
610 trusion Using Controlled Building Pressure, *Environmental Science &*  
611 *Technology* 46 (2012) 4792–4799.
- 612 [19] E. Jones, T. Oliphant, Pearu Peterson, SciPy: Open source scientific  
613 tools for Python, 2011.
- 614 [20] R. Shen, K. G. Pennell, E. M. Suuberg, Influence of Soil Moisture  
615 on Soil Gas Vapor Concentration for Vapor Intrusion, *Environmental*  
616 *Engineering Science* 30 (2013) 628–637.
- 617 [21] Y. Yao, Y. Wang, Z. Zhong, M. Tang, E. M. Suuberg, Investigating  
618 the Role of Soil Texture in Vapor Intrusion from Groundwater Sources,  
619 *Journal of Environmental Quality* 46 (2017) 776–784.
- 620 [22] Y. Yao, F. Mao, S. Ma, Y. Yao, E. M. Suuberg, X. Tang, Three-  
621 Dimensional Simulation of Land Drains as a Preferential Pathway for  
622 Vapor Intrusion into Buildings, *Journal of Environmental Quality* 46  
623 (2017) 1424–1433.
- 624 [23] L. A. Richards, Capillary conduction of liquids through porous mediums,  
625 *Physics* 1 (1931) 318–333.
- 626 [24] M. T. van Genuchten, A Closed-form Equation for Predicting the Hy-  
627 draulic Conductivity of Unsaturated Soils, *Soil Science Society of Amer-*  
628 *ican* 44 (1980) 892–898.
- 629 [25] R. J. Millington, J. P. Quirk, Permeability of porous solids, *Transactions*  
630 *of the Faraday Society* 57 (1961) 1200.
- 631 [26] H.-C. Dan, P. Xin, L. Li, L. Li, D. Lockington, Capillary effect on flow  
632 in the drainage layer of highway pavement, *Canadian Journal of Civil*  
633 *Engineering* 39 (2012) 654–666.
- 634 [27] L. D. V. Abreu, H. Schuver, Conceptual Model Scenarios for the Vapor  
635 Intrusion Pathway, 2012.

- 636 [28] U.S. Environmental Protection Agency, Users's Guide For Evaluating  
637 Subsurface Vapor Intrusion Into Buildings, 2004.
- 638 [29] U.S. EPA, Exposure Factors Handbook 2011 Edition, Technical Report,  
639 U.S. Environmental Protection Agency, 2011.
- 640 [30] M. D. Koontz, H. E. Rector, Estimation of Distributions for Residential  
641 Air Exchange Rates, Technical Report, U.S. Environmental Protection  
642 Agency, 1995.